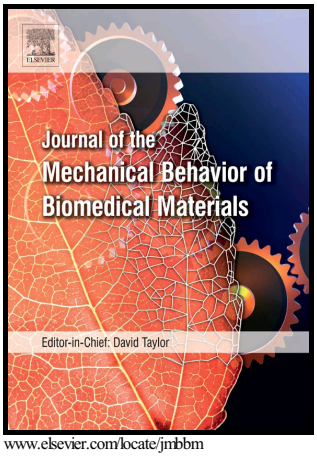

www.elsevier.com/locate/jmbbm

Characterisation of the mechanical properties of infarcted myocardium in the rat under biaxial tension and uniaxial compression

Mazin S. Sirry, J. Ryan Butler, Sourav S. Patnaik, Bryn Brazile, Robbin Bertucci, Andrew Claude, Ron McLaughlin, Neil H. Davies, Jun Liao, Thomas Franz

PII: S1751-6161(16)30205-3
DOI: http://dx.doi.org/10.1016/j.jmbbm.2016.06.029
Reference: JMBBM1980

To appear in: *Journal of the Mechanical Behavior of Biomedical Materials*

Received date: 14 March 2016
Revised date: 20 June 2016
Accepted date: 29 June 2016

Cite this article as: Mazin S. Sirry, J. Ryan Butler, Sourav S. Patnaik, Bryı Brazile, Robbin Bertucci, Andrew Claude, Ron McLaughlin, Neil H. Davies, Jur Liao and Thomas Franz, Characterisation of the mechanical properties o infarcted myocardium in the rat under biaxial tension and uniaxial compressior *Journal of the Mechanical Behavior of Biomedical Materials* http://dx.doi.org/10.1016/j.jmbbm.2016.06.029

Research Article

Characterisation of the mechanical properties of infarcted myocardium in the rat under biaxial tension and uniaxial compression

Mazin S. Sirry[1,2], J. Ryan Butler[3], Sourav S. Patnaik[4], Bryn Brazile[4], Robbin Bertucci[4], Andrew Claude[3], Ron McLaughlin[3], Neil H. Davies[5], Jun Liao[4], Thomas Franz[1,6,7*]

[1]Division of Biomedical Engineering, Department of Human Biology, University of Cape Town, Observatory 7925, South Africa

[2]Department of Biomedical Engineering, University of Medical Sciences and Technology, P.O. Box 12810, Khartoum, Sudan

[3]Department of Clinical Sciences, College of Veterinary Medicine, Mississippi State University, Mississippi, MS 39762, USA

[4]Tissue Bioengineering Laboratory, Department of Agricultural and Biological Engineering, Mississippi State University, Mississippi, MS 39762, USA

[5]Cardiovascular Research Unit, Chris Barnard Division of Cardiothoracic Surgery, University of Cape Town, Observatory 7925, South Africa

[6]Centre for High Performance Computing, Rosebank 7700, South Africa

[7]Bioengineering Science Research Group, Engineering Sciences, Faculty of Engineering and the Environment, University of Southampton, Southampton SO171BJ, UK

*Send correspondence to:
Thomas Franz, PhD
Department of Human Biology
Faculty of Health Sciences
University of Cape Town
Private Bag X3, Observatory 7935, South Africa
Tel: +27 21 650 1795
Fax: +27 21 448 7226
E-mail: thomas.franz@uct.ac.za

Abstract

Understanding the passive mechanical properties of infarcted tissue at different healing stages is essential to explore the emerging biomaterial injection-based therapy for myocardial infarction (MI). Although rats have been widely used as animal models in such investigations, the data in literature that quantify the passive mechanical properties of rat heart infarcts is very limited. MI was induced in rats and hearts were harvested immediately (0 day), 7, 14 and 28 days after infarction onset. Left ventricle anterioapical samples were cut and underwent equibiaxial and non equibiaxial tension followed by uniaxial compression mechanical tests. Histological analysis was conducted to confirm MI and to quantify the size of the induced infarcts. Infarcts maintained anisotropy and the nonlinear biaxial and compressive mechanical behaviour throughout the healing phases with the circumferential direction being stiffer than the longitudinal direction. Mechanical coupling was observed between the two axes in all infarct groups. The 0, 7, 14 and 28 days infarcts showed 438, 693, 1048 and 1218 kPa circumferential tensile moduli. The 28 day infarct group showed a significantly higher compressive modulus compared to the other infarct groups ($p= 0.0060$, 0.0293, and 0.0268 for 0, 7 and 14 days groups). Collagen fibres were found to align in a preferred direction for all infarct groups supporting the observed mechanical anisotropy. The presented data are useful for developing material models for healing infarcts and for setting a baseline for future assessment of emerging mechanical-based MI therapies.

Keywords:

Myocardial infarction, mechanical testing, rat, biaxial, compression, collagen

1 Introduction

Myocardial infarction (MI) is the most common cause of heart failure [1, 2]. Despite the currently available therapies, MI progression into heart failure is still a demanding problem. Cardiac transplantation is considered the only efficient cure for patients with severe heart failure. However, it is constrained by the availability of donors, the high cost, the limited capacity of the specialized clinics and lifelong immunosuppression [3]. Research has recently been devoted to exploring a promising new therapy for MI based on intramyocardial injection of a biomaterial [4-8].

The infarcted myocardium heals by formation of scar tissue which in turn expands with time. As the heart continues to pump, the non-contractile scar tissue stretches passively. The left ventricle (LV) wall tends to undergo structural changes that lead to dilation and increase in ventricular volume and pressure [9]. This long term consequence is called ventricular remodelling, a condition that can lead to a heart failure [10]. The functioning of a heart following an MI is strongly influenced by the mechanics of the infarcted tissue. Understanding the passive mechanical properties of infarcted tissue at different infarct stages is essential for improving the emerging biomaterial injection treatments for MI. Additionally, capturing the mechanical properties of infarcted tissue allows the development of constitutive models for computational studies.

The orientation of myofibres causes the myocardial tissue to exhibit mechanical anisotropy [11]. As such, uniaxial tensile testing is not sufficient in capturing the 3D constitutive behaviour of cardiac tissue even when applied individually in the principal material directions [12]. Biaxial tensile testing has been commonly utilized in characterization of soft tissues; such as myocardium [13], valve leaflets [14, 15] and pericardium [16].

One of the earliest attempt to investigate the biaxial mechanical properties of infarcted myocardium was presented by Gupta et al. [17]. They induced anterioapical MI in sheep hearts by ligating the left anterior descending (LAD) and second diagonal coronary arteries. Hearts were harvested at 4 hours, 1, 2 and 6 weeks after coronary ligation and biaxial tensile load was applied along the cardiac circumferential and longitudinal directions. Gundiah et al. [18] also studied the biaxial mechanical properties of healing MI in sheep hearts, however, they tested the infarcts at 2 and 8 months following the infarction onset.

Rats have been widely used as animal models in research of MI biomaterial injection therapy [5, 7, 19]. Yet, the available data in literature that quantifies the passive mechanical properties of infarcted rat myocardial tissue is very limited. Such data are essential to establish a baseline for experimental and computational assessment of the mechanical properties of the infarcted tissue in the context of biomaterial injection treatment. To the best of our knowledge, the rat myocardial infarcts were mechanically characterized in only one study by Fomovsky and Holmes [20] and therefore demanding characterization of further mechanical properties; such as compression stiffness and the in-plane mechanical coupling of rat infarct.

In this paper we investigated the passive mechanical properties of the healing infarcts in rat hearts using multiple loading protocols: equibiaxal and non-equibiaxial tension, and compression. Anterioapical MI was experimentally induced through LAD coronary ligation. Infarct samples were obtained at different post-infarct time points and tested under planar biaxial tension and uniaxial compression, respectively. In addition to improve the understanding of the mechanical behaviour of infarcted rat myocardium, this study aimed at providing additional data for potential future development of constitutive parameters for infarcts at different healing stages.

2 Materials and Methods

2.1 Myocardial infarction induction

The animal experiments were approved by the Mississippi State University Institutional Review Board and Institutional Animal Care and Use Committee and were performed in accordance with the National Institutes of Health (NIH, Bethesda, MD, USA) guidelines. Surgical procedures were performed according to Huang et al. [21]. Male Wistar rats (215-280g) were anaesthetized with a mixture of oxygen and 5.0% Isoflurane and intubated with a 16G intravenous catheter. Body temperature was maintained by placing rats on a heated operating pad. Positive-pressure ventilation was established and anaesthesia was maintained with a mix of oxygen/2.0% Isoflurane. A left thoracotomy was performed at the 4th intercostal space and ribs were retracted followed by a pericardiotomy. MI was induced by permanent ligation of LAD coronary artery with a 6-0 non-absorbable Polypropylene ligature 2-3 mm distal to the auricular appendix. The effectiveness of MI induction was assessed by the extent of paleness and fibrillation of the myocardial tissue on the anterior ventricular wall. Animals were euthanized by arresting the heart via intracardiac injection of saturated potassium chloride solution and hearts were harvested and stored in phosphate buffered saline (PBS) at 4 °C.

Infarcted hearts were harvested immediately (0 day), 7, 14 and 28 days after infarct induction (n= 5, 9, 9 and 9 respectively) representing several healing stages. For the animals of 7d, 14d and 28d groups, the chest was orderly closed and the animal was given subcutaneous buprenorphine injection for postoperative pain management.

2.2 Heart dissection and testing sample preparation

The harvested hearts were dissected to prepare testing samples. The atria, pulmonary trunk and the free wall of the right ventricle were cut away. A longitudinal cut was made through the

posterior wall of the LV from the base to apex. The LV was unfolded and a square sample (~10×10 mm) was dissected from the anterioapical region of the LV wall. All mechanical tests were carried out within 7 hours after harvesting the hearts. Samples were always kept moisturized during manipulation by continuously applying PBS.

2.3 Biaxial tensile test

The biaxial mechanical properties of myocardial tissue samples were captured using a biaxial testing system [15]. The length, width and thickness of samples were measured using a Vernier calliper and recorded prior to testing. For a single sample, 3 thickness measurements were made and the average was taken. Four optical markers were glued to the epicardial surface of the sample marking a ~ 4×4 mm area in the centre. Two evenly spaced suture needles were placed on each side of the sample ~2 mm away from the edge.

All biaxial tests were performed with tissue samples completely submerged in 37 °C PBS. Biaxial tensile load was applied along the cardiac circumferential and longitudinal directions of the sample at 0.5 mm/s. Following 10 preconditioning cycles of 30 N/m (force per unit length of the sample) equibiaxial tension, three protocols with different circumferential to longitudinal loading ratios were applied subsequently: Equibiaxial tension of 60:60 N/m, non-equibiaxial tension of 30:60 N/m and non-equibiaxial tension of 60:30 N/m. To quantify the tensile stiffness in the two material axes, circumferential and longitudinal tensile moduli were calculated from the steep region of the equibiaxial stress-strain curve of each sample.

The two non-equibiaxial loading protocols were introduced to examine the in-plane mechanical coupling between the circumferential and longitudinal axes and to provide the sufficient amount of data for the constitutive modelling. The mechanical coupling was examined by assessing the effect of increasing the tension in one axis on the extensibility of the other axis [14, 22].

2.4 Uniaxial compression test

Following the biaxial test, tissue samples underwent transmural compression testing, up to 30% of the sample thickness, using a uniaxial testing System (Mach-1, Biosyntech, MN, USA). The compression was applied at the 4 locations of optical markers using a plate indenter of 2.7 mm diameter while sample submerged in PBS. Each marker spot was preloaded to 1 g, preconditioned for 10 cycles, re-preloaded to 1 g and then loaded to 30% of compressive strain. Compression load was applied at rate of $T/10$ m/s, where T is the sample thickness. This is equivalent to strain rate of 0.1/s independent of the specimen thickness.

Compressive stress-strain data was obtained for the different infarct groups. The compressive moduli were calculated from the slope of the stress-strain curve at the region bounded by 25% and 30% of compressive strain.

2.5 Histology

Following mechanical testing, the infarcted tissue samples of the 7, 14 and 28 day groups were fixed in 4% paraformaldehyde for 48 hours and then in 70% ethanol. These samples underwent histology analysis to quantify the size of the induced infarct and analyse the orientation of collagen fibres.

The tissue portion above the ligation site was cut away since it has no significance in the infarct analysis. The sample was then cut into 4 equal circumferentially-adjacent blocks . The blocks were processed through graded alcohols (Illovo Sugar Ltd., Durban, South Africa) xylene (Saarchem, Gauteng, South Africa) and infiltrated with paraffin wax using the Tissue-Tek Rotary Tissue Processor (Sakura Finetek, Tokyo, Japan). After that, tissue blocks were embedded in paraffin wax (Merck KGaA, Darmstadt, Germany) and 2 sections of 4 µm were cut from the radial-longitudinal surface of each block , i.e. 8 sections per sample, at 0 and 120

µm using a Rotary Microtome HM360 (Microm, Waldorf,Germany). Sections were picked up on glass slides (Marienfeld GmbH & Co. KG, Lauda-Königshofen, Germany) and baked on a hot plate at 60 °C (Kunz Instruments AB, Nynäshamn, Sweden) for 30 minutes before being dewaxed in xylene and hydrated through graded alcohols down to water. Tissue sections were then stained using Masson's trichrome to distinguish the collagen fibres from myocytes in the tissue. A 0.5% Acid Fuchsin solution (Merck KGaA, Darmstadt, Germany) was applied for 5 min and rinsed in tap water. Excess Acid Fuchsin was removed by applying 1% Phosphomolybdic acid solution (SigmaeAldrich Chemie GmbH, Steinheim, Germany) for 5min. The slides were then washed in water and counterstained for 2 min with 2% Light Green SF Yellowish (Sigma Aldrich Chemie GmbH, Steinheim, Germany) before they were dehydrated through alcohol, cleared with xylene and mounted with Entellan (Merck KGaA, Darmstadt, Germany).

In order to analyse the orientation of collagen fibres, the tissue block representing the middle region of the sample was sectioned parallel to the epicardial surface, i.e. at the circumferential-longitudinal plane. Ten sections of 7 µm thickness were obtained from each sample at equally spaced transmural depths and stained with picrosirius red.

2.6 Infarct size quantification

Images of Masson's trichrome sections were acquired using Eclipse 90i microscope with DXM-1200C digital camera (Nikon Corporation, Tokyo, Japan) at 2 × magnification and stitched (NIS Elements BR 3.0, Nikon Corporation). Digital images of tissue sections were imported in Visiopharm Integrator System (Visiopharm, Hørsholm, Denmark) for analysis. The infarct and intact areas, characterized by the presence of collagen and cardiomyocyte respectively, were measured in each section using an unsupervised image analysis. The analysis involved an

automated segmentation of collagen and myocytes regions in the image using coloured spatial masks. The percentages of the infarct and intact areas in the individual sections were calculated. The overall infarct size of a sample was estimated by normalizing the sum of infarct areas in the 8 sections by the sum of the entire section areas. Samples that exhibited less than 40% infarction were excluded from the study. This threshold was determined so as to ensure a transmural and adequate circumferential and longitudinal extend of the infarct and based on the analysis of the sets of infarcted hearts presented in this study

2.7 Analysis of collagen fibres orientation

The analysis of collagen orientation was performed following the approach described by Fomovsky and Holmes [20]. In brief, images of picrosirius red sections were acquired using Eclipse 90i polarizing microscope with DXM-1200C digital camera (8 bit, monochrome, 1024 × 1280 pixels) at 10 × magnification. For each section, a bright-field image and a polarized image were obtained. The bright-field image was subtracted from the polarized image to isolate the collagen fibres. The collagen orientation was analysed in the subtraction image using MatFiber [20], a custom-written MATLAB script. The script measured the orientation in finite subregions of the image. In the current study, images were devided into subregions of 50 × 50 pixels.

2.8 Statistical analysis

The experimental data were presented as mean ± standard deviation (SD). The statistical analysis was performed using one-way analysis of variances (ANOVA) followed by Fisher least square deviation (LSD) multiple comparison post-hoc test between groups (STATISTICA 12, StatSoft, Inc., Tulsa, USA). The differences were considered statistically significant when $p<0.05$.

3 Results

3.1 Visual inspection of harvested hearts

By visual inspection of the harvested hearts, the 0d infarct hearts did not show noticeable changes and thus distinguishing the infarct zone was not applicable. However, the infarct zone was clearly visible on the hearts of 7, 14 and 28d groups as shown in Figure 1. The infarct zone extended distal to the ligation site. The damaged tissue appeared in a pale colour which was distinguishable from the red/brown colour of the surrounding intact myocardium. A loss in the muscle tone and wall thinning were also a characteristic of the infarcted tissue in contrast to the intact myocardium.

3.2 Infarct size

Staining the tissue sections of the infarcted samples with Masson's trichrome distinguished the collagen fibres from myocytes. The collagen appeared blue while myocytes appeared red as illustrated in Figure 2 (a). As a result of segmentation in Visiopharm, Figure 2 (b), the collagen and myocytes were covered with blue and green masks, respectively. As such, the area of these masks represented the areas of the infarct and intact tissue in a section.

The histogram in Figure 2 (c) shows the distribution of infarct in the individual sections of samples for different groups. The infarcted area was presented as percentage of the entire section area. For illustration purposes, the samples in each group were numbered from 1 to 9 while sections were numbered from 1 to 8. Some samples were fully intact, i.e. 0% infarct, indicating an unsuccessful MI induction, e.g. Sample 2 at 7d, Sample 7 at 14d and Sample 1 at 28d. No sample showed infarction in all of the 8 sections; the maximum was 7 sections. The estimated infarct size in samples is shown in Figure 2 (d).

3.3 Equibiaxial tension

The biaxial tensile testing of some samples failed due to technical issues producing incomplete mechanical data. These samples were excluded from the study. The final number of samples that underwent all loading protocols of biaxial testing and were included in the data analysis was n = 5 (0d), 5 (7d), 3 (14d) and 4 (28d).

The stress-strain relationship of the equibiaxial tensile tests for different infarct groups is shown in Figure 3. In general, all infarct groups exhibited an anisotropic nonlinear behaviour in which the circumferential direction was stiffer than the longitudinal direction. However, the 0 and 7d groups, Figure 3 (a, b) respectively, showed an isotropic behaviour at lower strain (up to ~0.07 for 0d and ~0.05 for 7d). The degree of anisotropy in the 14d infarct group, Figure 3 (c), was more pronounced compared to the other groups as graphically indicated by the gap between the biaxial curves.

The mean tensile modulus, shown in in Figure 4, was calculated for the different infarct groups as an indication for infarct stiffness. In the circumferential direction, Figure 4 (a), the moduli for 0d, 7d, 14d and 28d groups was found to be 438, 693, 1048 and 1218 kPa, respectively. The stiffness increased in proportion to the increasing time after coronary ligation. The modulus of the 28d was significantly higher compared to the 0d and 7d infarct ($p=0.0038$ and $p=0.0343$ respectively). The modulus of the 14d infarcts was also significantly higher than the 0d infarct ($p=0.0253$). In the longitudinal direction, Figure 4 (b), the infarcts at 0, 7 and 14 days exhibited moduli of 247, 250 and 212 kPa, respectively. At 28 day an increase in the stiffness was observed (487 kPa), yet statistically not significant.

3.4 Non-equibiaxial tension

The stress-strain relationship of the 30:60 biaxial test for different infarct groups is shown in Figure 5. All infarct groups exhibited negative circumferential strain due to the in-plane mechanical coupling between the two axes. The variation in the circumferential extensibility between infarct groups was very limited compared to the longitudinal extensibility.

The stress-strain graphs from the 60:30 loading protocol are shown in Figure 6. A varying level of anisotropy was observed among the infarct groups. As the infarct progressed with time, the level of anisotropy gradually decreased until it became nearly isotropic at 28 day. Negative strains were observed in the 0 and 7d groups only.

The in-plane mechanical coupling between the circumferential and longitudinal direction of infarcts was assessed by comparing the change in extensibility in one direction as the load increases in the other direction. Figure 7 illustrates the change in peak strain in one direction as the tension changes in the other direction. For example, the 7d infarct exhibited 23% decrease in the circumferential strain when the longitudinal tension was increased from 30 (in the 60:30 protocol) to 60 N/m (in the 60:60 protocol) as shown in Figure 7 (a). However, the longitudinal strain of the same group decreased by 36% when the circumferential tension was increased from 30 (in the 30:60 protocol) to 60 N/m (in the 60:60 protocol). The mechanical coupling in 0 and 14d groups was nearly symmetric, i.e. equal change in directional strain, whereas asymmetric mechanical coupling was observed for 7 and 28d groups. The strongest mechanical coupling (40%) was observed in the circumferential direction of the 28d group with negligible change in the longitudinal strain. This indicates that the longitudinal axis had a stronger mechanical effect on the circumferential axis in the 28d infarct.

3.5 Compression

Erratic compression measurements from some samples were excluded from the study. Several compression measurements were obtained from a single sample. The total number of measurements obtained for each infarct group was n = 5 (0d), 6 (7d), 8 (14d) and 6 (28d).

Figure 8 illustrates the compressive mechanical properties of the infarcted myocardium. All infarct groups exhibited a non-linear compressive stress-strain behaviour as shown in Figure 8 (a). Up to 10% of compressive strain, a similar linear stress-strain behaviour was observed. Variation between groups became more pronounce as the strain exceeded 20%.

The compressive moduli, shown in Figure 8 (b), was found to be 145, 247, 260 and 522 kPa for 0d, 7d, 14d and 28d infarct groups. The 28d infarct group showed a significantly higher compressive modulus compared to 0, 7 and 14d infarct groups ($p= 0.0060$, 0.0293, and 0.0268, respectively).

3.6 Orientation of collagen fibres

Collagen orientation was analysed in individual tissue sections from different infarct samples as illustrated in Figure 9 (a). Analysis was failed in some samples. The final number of samples underwent collagen orientation analysis was n = 4 (7d), 2 (14d) and 3 (28d). Fibre angles from each tissue section were measured for all samples of the different infarct groups. The graph in Figure 9 (b) illustrates the mean collagen orientation at 10 transmural sections for the 7, 14 and 28 days infarct groups. The three infarct groups showed close trend with 14 days appeared with slightly more circumferential orientation in the mid-wall sections.

Figure 10 (a) illustrates the overall mean fibre angle calculated for 7, 14 and 28 days infarct groups. All infarct groups exhibited a close mean angle with the 14d infarcts showing a slightly

more horizontal orientation. The mean vector length (MVL) was calculated for each infarct group as a measure of fibres alignment. The degree of fibres alignment was highest in the 7d group (MVL=0.85) compared to the two other infarct groups. The histograms in Figure 10 (b, c and d) provides an insight into the overall angular distribution of collagen fibres in different infarct groups. The 7d infarcts showed a single peak whereas the 14d and 28d infarcts showed double peak. More circumferential fibres (i.e. around 0°) can be observed in 14d infarcts compared with the other groups.

4 Discussion

This study investigated the mechanical behaviour of rat infarcted myocardium under different loading conditions taking into account the temporal change in mechanical properties of healing infarcts. The infarcted hearts were explanted immediately, 7, 14 and 28 days after LAD coronary artery ligation. Infarct samples underwent planar equibiaxial and non-equibiaxial tensile tests followed by wall compression test. Individual samples underwent structural analysis to quantify the infarct size and to determine the orientation of collagen fibres. Infarcts were found to maintain anisotropy and nonlinear biaxial and compressive mechanical behaviour throughout the healing phases. The observed anisotropic mechanical behaviour of infarcts, with the circumferential direction being stiffer than the longitudinal, was supported by the alignment of collagen. Mechanical coupling was observed between the two axes in all infarct groups. With progression of infarct healing, the increase in the circumferential and compressive stiffness was more significant than the increase in longitudinal stiffness.

4.1 Induction of myocardial infarction

In vivo MI induction in rats is a challenging procedure due to some commonly known factors. These include the small size of a rat heart, the small exposure site and the difficulty in

maintaining a consistent infarct size. The latter is a crucial factor when aiming at mechanically testing the infarct. Ideally, the testing sample should be 100% infarcted to precisely capture the mechanical properties of the infarct.

In the current experiments, we aimed at inducing successful and large infarcts by using multiple ligation sites, Figure 1 (a), instead of a single site and by increasing the size (depth) of the occluded region as proposed by Huang et al. [21]. Yet no samples from the 7, 14 or 28 day groups was 100% infarcted. Furthermore, MI induction was completely unsuccessful in some samples yielding 0% infarct size (Figure 2) and produced relatively small infarct sizes such as 4, 9 and 12% in other samples. This highlights the difficulty to control the infarct size or maintain its consistency among infarct groups. It also emphasizes the need to carefully quantify the infarct size within individual samples and take this into account when interpreting the outcomes of mechanical testing.

4.2 Quantification of infarct size and thresholding

The histology analysis was performed following mechanical testing to examine the consistency of the induced infarcts. In order to provide an adequate estimate of the infarcted region in a sample, histology-based measurement of the infarcted area was applied in 8 equidistant parallel sections of the testing sample. MI studies that involve experimental infarcts in rodent models usually followed two common histology-based approaches to estimate the infarct size in the LV: (1) measuring the area of the infarcted region [23-25] or (2) measuring the arc length of the infarcted region [7, 26]. The area-based method is often used with early stage infarcts. However, the wall thinning associated with the late stage infarcts makes the length-based method more suitable [27]. Although the current study involved chronic infarcts (i.e. 7, 14 and 28 days infarcts), the area-based method was utilized. Unlike other studies in which infarct size was

measured in the entire LV, the infarct size in the current study was measured in the sample only. The sample represented a small portion of the LV where the infarct would most likely lie. As such, even though a sample experienced wall thinning, the thickness was uniform in the whole sample. Furthermore, the area-based method was more accurate and limited the subjectivity. Applying this method at 8 equally spaced sections provided an adequate estimate of the infarct size and infarct spatial spreading on a sample.

Following the histological analysis of infarct samples, an infarct size threshold of 40% was determined below which a sample was considered poorly infarcted and excluded from the study. The motivation for obtaining this threshold originated from the fact that no sample from the chronic infarct groups was 100% infarcted, Figure 2 (b). As such, it was necessary to ensure that the entire central target region of the biaxial testing samples [14] contained as much properly infarcted tissue as possible. The histogram of the infarcted area in individual sections, Figure 2 (a), provides information on the distribution of the infarct both circumferentially and longitudinally. All samples were cut at the ligation site prior to histology analysis. Therefore, a single bar in the histogram demonstrates how far the infarct in that particular section extends in the longitudinal direction. The 8 bars of a sample represent equally spaced longitudinal sections and thus together illustrate how far the infarct extends circumferentially. Examining the histology images and the in-plane extension of the infarct, 40% was found to be the minimum infarct size required to ensure a transmural and adequate circumferential and longitudinal extend of the infarct.

By eliminating samples that exhibited less than 40%, the chance that the mechanical properties were captured from properly infarcted target region was considerably increased. This was also confirmed for the compression data since compressive loads were applied at the optical markers which were located in the target region. It is important, however, to note that the 40% value was

obtained based on the analysis of the sets of infarcted hearts presented in this study and is not necessary suitable for other studies.

The infarct size in the immediate (i.e. 0d) group was not quantified in this study. Collagen starts accumulating in infarcted tissue at 2 days after infarction onset [28]. Therefore, Masson's trichrome staining was not suitable for this group since the infarcted hearts were harvested few minutes after coronary ligation. Triphenyltetrazolium chloride (TTC) staining is a macroscopic approach widely used to identify early phase post-mortem infarcted myocardial tissue [29, 30]. In a pilot study on the 0d infarcts, TTC staining did not identify the infarcts after biaxial testing although successfully did so on samples that did not undergo biaxial testing. The major causes of this observation were not yet fully understood. Nevertheless, all hearts from the 0d group were assumed to be properly infarcted and thus included in the study. This assumption was based on a key argument. Since the heart was to be harvested immediately, a lengthy thoracotomy was made during operation and the heart was openly exposed allowing comfortable access to the LAD coronary artery. As such, the MI in this group was induced with high certainty providing a consistent mechanical properties as illustrated by the relatively small standard deviation in this group, Figure 3 (a).

4.5 Mechanical properties of infarcts

Our study showed that infarcts maintain the non-linear anisotropic mechanical behaviour throughout the different healing stages with varying degree of anisotropy (Figure 3). This was not only observed on the mean stress-strain relationships, but was also observed in stress-strain curves of individual samples of different infarct groups (see Figure 1 to 4 in Sirry et al. [31]). These findings agreed with previous studies in which anisotropic behaviour of the infarcted tissue under equibiaxial tension was also observed in sheep hearts [17, 18]. Collagen is the major

determinant of the mechanical properties of the infarcted myocardium [32, 33]. In particular, the degree of anisotropy is primarily determined by the alignment of the collagen fibres although isolated muscle fibres have an effect [17]. In the current study, the mechanical anisotropy exhibited by the healing infarcts was supported by the alignment of collagen orientation. Collagen fibres were found to mostly align around -45° in the different infarct groups. The highly aligned collagen fibres (around ca. -45°) observed for the 7d infarcts with MVL=0.85, Figure 10 (a, b), could possibly explain the isotropy at low strains and the small degree of anisotropy at higher strains observed for this group, Figure 3 (b); the collagen fibres tended to align centrally with respect to the directions of the biaxial load which was applied at 0° and 90°. The pronounced anisotropy observed for the 14d infarct group, Figure 3 (c), can be attributed to the larger number of horizontally oriented collagen, Figure 9 (b) and Figure 10 (a), compared to the other chronic infarcts. Fomovsky and Holmes [20] argued that healing rat infarcts were isotropic both structurally and mechanically which indicates disagreement with the findings of our study. Although Clarke et al. [34] recently suggested that the collagen fibre structure and the mechanical properties of infarcted tissue could vary between studies employing the same animal model, the reason behind this variation is not very well understood. Nevertheless, the discrepancy between our results and that of Fomovsky and Holmes [20] could potentially be attributed to the difference in animal strain [35, 36]. It could also be due to the variation in the amount of isolated muscle fibres especially when considering the difficulty of precisely controlling the size of the infarct in the samples as we demonstrated in this study. Furthermore, the orientation of collagen was shown to vary according to the location of the infarct in the LV of a rat [37]; the collagen in a mid-ventricle infarct aligns mostly in the circumferential direction whereas collagen fibres are randomly oriented in an apical infarct. All or some of these factors

may have contributed in the discrepancy between the two studies. This situation highlights the demand for further investigations in order to provide adequate explanation.

The orientation of collagen is also believed to play a major role in the mechanical coupling observed between material axes when infarcts are subjected to non-equibiaxial tension (Figure 7). Mechanical coupling has been reported for several biological soft tissues such as; myocardium [22, 38], pericardium [39], valve leaflet [14] and urinary bladder [40]. The exact underlying mechanism which causes this phenomena is not clear although some hypothesis attributed it to the dynamic change of collagen orientation in response to the unequal biaxial loading [14, 41]. Nevertheless, the non-equibiaxial experiment presented in this study could potentially be helpful in identifying material parameters for the different infarct phases.

The increase in the circumferential, Figure 4 (a), and compressive, Figure 8, stiffness of the healing infarcts with time is attributed to the accompanying increase in collagen deposition and cross-linking [32, 42]. While the compressive stiffness is related to the content of collagen, the directional stiffness is predominantly controlled by the degree of alignment of the deposited collagen. For example, the change in the longitudinal stiffness, Figure 4 (b), with increasing healing time, though not statistically significant, could be attributed to the circumferential alignment of the accumulated collagen. These arguments are supported with the collagen content and orientation found in rat infarcts at 1 and 6 weeks after infarction reported by Fomovsky and Holmes [20] where the increase in collagen content at 6 weeks compared to 1 week was found to be remarkable, however, the increase in the content of the longitudinal aligned collagen is very small compared to that of the circumferential collagen. Therefore, the circumferential stiffness of the infarct at 28 and 14 days was significantly higher compared to earlier infarct stages.

5 Conclusions

We comprehensively characterized the mechanical properties of healing infarcts in a rat model for up to one month after the infarction onset. Healing infarcts in rat hearts exhibited nonlinear and anisotropic mechanical behaviour accompanied by in-plane mechanical coupling between the two principal axes. The circumferential direction was stiffer than the longitudinal direction. The degree of anisotropy may vary between healing stages according to the amount of load and the orientation of the deposited collagen. The latter is believed to play a major role in inducing the mechanical coupling. As the infarct healing progresses, the circumferential and compressive stiffness increases more pronouncedly compared to the longitudinal stiffness. The presented data can be employed to develop material models of healing infarcts towards computational investigations of the mechanical aspects of MI and its emerging therapies in rat models.

Acknowledgements

The authors would like to thank Prof Jeffrey W. Holmes from Robert M. Berne Cardiovascular Research Center, University of Virginia, for his helpful and constructive comments that greatly contributed to improving the final version of the paper. The authors would like to also thank Mrs. Nancy Pounds and Mrs. Jamie Walker from the College of Veterinary Medicine, Mississippi State University, for the help with the anaesthesia and operation room management. This study was supported financially by the National Research Foundation (NRF) of South Africa and the Centre for High Performance Computing, Council for Scientific and Industrial Research, South Africa. Any opinion, findings and conclusions or recommendations expressed in this publication are those of the authors and therefore the NRF does not accept any liability in regard thereto. MSS acknowledges the International Society of Biomechanics Matching

Dissertation Grant. NHD acknowledges financial support from the South African Medical Research Council.

Conflict of Interest Statement

The authors declare that they have no conflicts of interest.

References

1. AHA, *Heart disease and stroke statistics: Our guide to current statistics and the supplement to our heart and stroke facts.* 2008, American Heart Association: Dallas.
2. Rosamond W, Flegal K, Furie K, Go A, Greenlund K, Haase N, Hailpern SM, Ho M, Howard V, Kissela B, Kittner S, Lloyd-Jones D, McDermott M, Meigs J, Moy C, Nichol G, O'Donnell C, Roger V, Sorlie P, Steinberger J, Thom T, Wilson M, Hong Y. Heart disease and stroke statistics—2008 update: A report from the american heart association statistics committee and stroke statistics subcommittee. *Circulation* 2008; **117**:e25-e146. DOI:10.1161/circulationaha.107.187998.
3. Struck E, Hagl S, Meisner H, Sebening F. Heart transplantation: Limitations and perspectives. *Zeitschrift fur Kardiologie* 1985; **74 Suppl 6**:59-63.
4. Christman KL, Lee RJ. Biomaterials for the treatment of myocardial infarction. *Journal of the American College of Cardiology* 2006; **48**:907-913. DOI:10.1016/j.jacc.2006.06.005.
5. Dobner S, Bezuidenhout D, Govender P, Zilla P, Davies N. A synthetic non-degradable polyethylene glycol hydrogel retards adverse post-infarct left ventricular remodeling. *Journal of Cardiac Failure* 2009; **15**:629-636.
6. Ifkovits JL, Tous E, Minakawa M, Morita M, Robb JD, Koomalsingh KJ, Gorman JH, Gorman RC, Burdick JA. Injectable hydrogel properties influence infarct expansion and extent of postinfarction left ventricular remodeling in an ovine model. *Proceedings of the National Academy of Sciences* 2010; **107**:11507-11512. DOI:10.1073/pnas.1004097107.
7. Kadner K, Dobner S, Franz T, Bezuidenhout D, Sirry MS, Zilla P, Davies NH. The beneficial effects of deferred delivery on the efficiency of hydrogel therapy post myocardial infarction. *Biomaterials* 2012; **33**:2060-2066. DOI:10.1016/j.biomaterials.2011.11.031.
8. Sirry MS, Davies NH, Kadner K, Dubuis L, Saleh MG, Meintjes EM, Spottiswoode BS, Zilla P, Franz T. Micro-structurally detailed model of a therapeutic hydrogel injectate in a rat biventricular cardiac geometry for computational simulations. *Computer Methods in Biomechanics and Biomedical Engineering* 2015; **18**:325-331. DOI:10.1080/10255842.2013.793765.
9. Holmes JW, Borg TK, Covell JW. Structure and mechanics of healing myocardial infarcts. *Annual Review of Biomedical Engineering* 2005; **7**:223-253.
10. McMurray JJ, Pfeffer MA. Heart failure. *Lancet* 2005; **365**:1877-1889. DOI:10.1016/s0140-6736(05)66621-4.
11. Bovendeerd PHM, Arts T, Huyghe JM, van Campen DH, Reneman RS. Dependence of local left ventricular wall mechanics on myocardial fiber orientation: A model study. *Journal of Biomechanics* 1992; **25**:1129-1140. DOI:Doi: 10.1016/0021-9290(92)90069-d.

12. Usyk TP, McCulloch AD. *Computational methods for soft tissue biomechanics.*, in *Biomechanics of soft tissue in cardiovascular systems.*, Holzapfel, G A, Ogden, R W, Editors. 2003, Springer: Wien. p. 273-342.
13. Demer LL, Yin FC. Passive biaxial mechanical properties of isolated canine myocardium. *The Journal of Physiology* 1983; **339**:615-630.
14. Billiar KL, Sacks MS. Biaxial mechanical properties of the natural and glutaraldehyde treated aortic valve cusp--part i: Experimental results. *Journal of Biomechanical Engineering* 2000; **122**:23-30.
15. Grashow JS, Yoganathan AP, Sacks MS. Biaixal stress-stretch behavior of the mitral valve anterior leaflet at physiologic strain rates. *Annals of Biomedical Engineering* 2006; **34**:315-325. DOI:10.1007/s10439-005-9027-y.
16. Chew PH, Yin FCP, Zeger SL. Biaxial stress-strain properties of canine pericardium. *Journal of Molecular and Cellular Cardiology* 1986; **18**:567-578. DOI:Doi: 10.1016/s0022-2828(86)80965-8.
17. Gupta KB, Ratcliffe MB, Fallert MA, Edmunds LH, Bogen DK. Changes in passive mechanical stiffness of myocardial tissue with aneurysm formation. *Circulation* 1994; **89**:2315-2326. DOI:10.1161/01.cir.89.5.2315.
18. Gundiah N, Chang D, Zhang P, Ratcliffe M, Pruitt L, *Structural and mechanical characteristics of healing myocardial scar tissue*, in *ASME International Mechanical Engineering Congress and Exposition*. 2004: Anaheim, CA, USA. p. 265-266.
19. Landa N, Miller L, Feinberg MS, Holbova R, Shachar M, Freeman I, Cohen S, Leor J. Effect of injectable alginate implant on cardiac remodeling and function after recent and old infarcts in rat. *Circulation* 2008; **117**:1388-1396. DOI:10.1161/CIRCULATIONAHA.107.727420.
20. Fomovsky GM, Holmes JW. Evolution of scar structure, mechanics, and ventricular function after myocardial infarction in the rat. *American Journal of Physiology - Heart and Circulatory Physiology* 2010; **298**:H221-H228. DOI:10.1152/ajpheart.00495.2009.
21. Huang NF, Sievers RE, Park JS, Fang Q, Li S, Lee RJ. A rodent model of myocardial infarction for testing the efficacy of cells and polymers for myocardial reconstruction. *Nature Protocols* 2006; **1**:1596-1609.
22. Ghaemi H, Behdinan K, Spence AD. In vitro technique in estimation of passive mechanical properties of bovine heart: Part i. Experimental techniques and data. *Medical Engineering & Physics* 2009; **31**:76-82. DOI:DOI: 10.1016/j.medengphy.2008.04.008.
23. Park SW, Lee SY, Park SJ, Lee S-C, Gwon H-C, Kim D-K. Quantitative assessment of infarct size in vivo by myocardial contrast echocardiography in a murine acute myocardial infarction model. *International Journal of Cardiology* 2004; **97**:393-398. DOI:0.1016/j.ijcard.2003.10.034.
24. Piot CA, Padmanaban D, Ursell PC, Sievers RE, Wolfe CL. Ischemic preconditioning decreases apoptosis in rat hearts in vivo. *Circulation* 1997; **96**:1598-1604. DOI:10.1161/01.cir.96.5.1598.
25. Liu Z, Kastis GA, Stevenson GD, Barrett HH, Furenlid LR, Kupinski MA, Patton DD, Wilson DW. Quantitative analysis of acute myocardial infarct in rat hearts with ischemia-reperfusion using a high-resolution stationary spect system. *Journal of Nuclear Medicine* 2002; **43**:933-939.
26. Pfeffer MA, Pfeffer JM, Fishbein MC, Fletcher PJ, Spadaro J, Kloner RA, Braunwald E. Myocardial infarct size and ventricular function in rats. *Circulation Research* 1979; **44**:503-512. DOI:10.1161/01.res.44.4.503.

27. Takagawa J, Zhang Y, Wong ML, Sievers RE, Kapasi NK, Wang Y, Yeghiazarians Y, Lee RJ, Grossman W, Springer ML. *Myocardial infarct size measurement in the mouse chronic infarction model: Comparison of area- and length-based approaches*. Vol. 102. 2007. 2104-2111.
28. Cleutjens JPM, Blankesteijn WM, Daemen MJAP, Smits JFM. The infarcted myocardium: Simply dead tissue, or a lively target for therapeutic interventions. *Cardiovascular Research* 1999; **44**:232-241. DOI:10.1016/s0008-6363(99)00212-6.
29. Fishbein MC, Meerbaum S, Rit J, Lando U, Kanmatsuse K, Mercier JC, Corday E, Ganz W. Early phase acute myocardial infarct size quantification: Validation of the triphenyl tetrazolium chloride tissue enzyme staining technique. *American Heart Journal* 1981; **101**:593-600. DOI:10.1016/0002-8703(81)90226-X.
30. Khalil PN, Siebeck M, Huss R, Pollhammer M, Khalil MN, Neuhof C, Fritz H. Histochemical assessment of early myocardial infarction using 2,3,5-triphenyltetrazolium chloride in blood-perfused porcine hearts. *Journal of Pharmacological and Toxicological Methods* 2006; **54**:307-312. DOI:10.1016/j.vascn.2006.02.010.
31. Sirry MS, Butler JR, Patnaik SS, Brazile B, Bertucci R, Claude A, McLaughlin R, Davies NH, Liao J, Franz T. Mechanical properties and structure of infarcted myocardium in the rat under biaxial tension and uniaxial compression. *Data in Brief*; ***submitted***.
32. Cleutjens JP, Verluyten MJ, Smiths JF, Daemen MJ. Collagen remodeling after myocardial infarction in the rat heart. *American Journal of Pathology* 1995; **147**:325-338.
33. Fomovsky GM, Thomopoulos S, Holmes JW. Contribution of extracellular matrix to the mechanical properties of the heart. *Journal of Molecular and Cellular Cardiology* 2010; **48**:490-496. DOI:10.1016/j.yjmcc.2009.08.003.
34. Clarke SA, Richardson WJ, Holmes JW. Modifying the mechanics of healing infarcts: Is better the enemy of good? *Journal of Molecular and Cellular Cardiology*. DOI:10.1016/j.yjmcc.2015.11.028.
35. van den Borne SWM, van de Schans VAM, Strzelecka AE, Vervoort-Peters HTM, Lijnen PM, Cleutjens JPM, Smits JFM, Daemen MJAP, Janssen BJA, Blankesteijn WM. Mouse strain determines the outcome of wound healing after myocardial infarction. *Cardiovascular Research* 2009; **84**:273-282.
36. Walkin L, Herrick SE, Summers A, Brenchley PE, Hoff CM, Korstanje R, Margetts PJ. The role of mouse strain differences in the susceptibility to fibrosis: A systematic review. *Fibrogenesis and Tissue Repair* 2013; **6**:18-18. DOI:10.1186/1755-1536-6-18.
37. Fomovsky GM, Rouillard AD, Holmes JW. Regional mechanics determine collagen fiber structure in healing myocardial infarcts. *Journal of Molecular and Cellular Cardiology* 2012; **52**:1083-1090.
38. Yin FCP, Strumpf RK, Chew PH, Zeger SL. Quantification of the mechanical properties of noncontracting canine myocardium under simultaneous biaxial loading. *Journal of Biomechanics* 1987; **20**:577-589. DOI:10.1016/0021-9290(87)90279-x.
39. Sacks M, Chuong CJ. Orthotropic mechanical properties of chemically treated bovine pericardium. *Annals of Biomedical Engineering* 1998; **26**:892-902. DOI:10.1114/1.135.
40. Gilbert TW, Wognum S, Joyce EM, Freytes DO, Sacks MS, Badylak SF. Collagen fiber alignment and biaxial mechanical behavior of porcine urinary bladder derived extracellular matrix. *Biomaterials* 2008; **29**:4775-4782. DOI:10.1016/j.biomaterials.2008.08.022.
41. Yin FCP, Chew PH, Zeger SL. An approach to quantification of biaxial tissue stress-strain data. *Journal of Biomechanics* 1986; **19**:27-37. DOI:10.1016/0021-9290(86)90106-5.

42. Vivaldi MT, Eyre DR, Kloner RA, Schoen FJ. Effects of methylprednisolone on collagen biosynthesis in healing acute myocardial infarction. *The American Journal of Cardiology* 1987; **60**:424-425. DOI:10.1016/0002-9149(87)90277-3.

Figure Captions

Figure 1: Harvested infarcted hearts at 7 (a), 14 (b) and 28 days (c) after coronary artery ligation showing the infarcted tissue (dotted circle) and locations of ligating sutures (arrow).

Figure 2: Quantification of infarct size: (a) Histological micrograph of an infarcted tissue section stained with Masson's trichrome. Collagen appears blue and myocytes appears red. (b) Image after being segmented in Visiopharm. Blue and green masks represent collagen and myocytes respectively. (c) Histogram of the percentage of infarcted area in individual sections of tissue samples for 7, 14 and 28d groups. (d) Estimated infarct size in tissue samples of 7, 14 and 28 day infarct groups.

Figure 3: Mean stress-strain relationship from the 60:60 N/m biaxial tensile test for 0 (a), 7 (b), 14 (c) and 28 day (d) infarct group. Error bars represent SD and were partially presented for illustration purposes. * $p<0.05$. Raw data from equibiaxial testing of individual samples for different infarct groups can be obtained from Sirry et al. [31].

Figure 4: Mean circumferential (a) and longitudinal (b) tensile modulus for different infarct groups. Tensile moduli were calculated from the slope of the steep region of the equibiaxial stress-strain curves of individual samples. Error bars represent SD. * $p<0.05$. Circumferential and longitudinal tensile moduli of individual samples can be obtained from Sirry et al. [31].

Figure 5: Mean stress-strain relationship from 30:60 N/m biaxial tensile tests for 0 (a), 7 (b), 14 (c) and 28 day (d) infarct group. Error bars represent SD and were partially presented for illustration purposes.

Figure 6: Mean stress-strain relationship from 60:30 N/m biaxial tensile tests for 0 (a), 7 (b), 14 (c) and 28 day (d) infarct group. Error bars represent SD and were partially presented for illustration purposes.

Figure 7: Peak circumferential (a) and longitudinal (b) strain obtained from different loading protocols of the non-equibiaxial tensile tests demonstrating the effect of mechanical coupling. The percentage change in strain between loading protocols is indicated for each infarct group. Data are presented in mean and error pars represent SD.

Figure 8: Compressive mechanical properties of infarcted myocardium: (a) Mean compressive stress-strain relationship for different infarct groups. (b) Mean compressive modulus calculated for different infarct groups. Compressive moduli were calculated from the slope of the stress-strain curves at the region bounded by 25% and 30% of compressive strain. Error bars represent SD. * $p<0.05$. Raw data from compressive testing of individual samples can be obtained from Sirry et al. [31].

Figure 9: (a) Representative microscopic image of tissue section analysed by MatFiber [20] illustrating collagen orientation indicated by arrows. (b) Mean angle of collagen orientation at 10 transmural sections calculated for different infarct groups. S1 and S10 are the most epicardial and endocardial sections, respectively. Error bars represent circular SD and were partially presented for illustration purposes. Collagen orientation raw data can be obtained from Sirry et al. [31].

Figure 10: (a) Mean angle of collagen orientation in infarct groups. The error bars represent circular SD. MVL= mean vector length. Histogram of collagen orientation measured at subregions of tissue sections of the 7 (b) 14 (c) and 28 day (d) infarct groups.

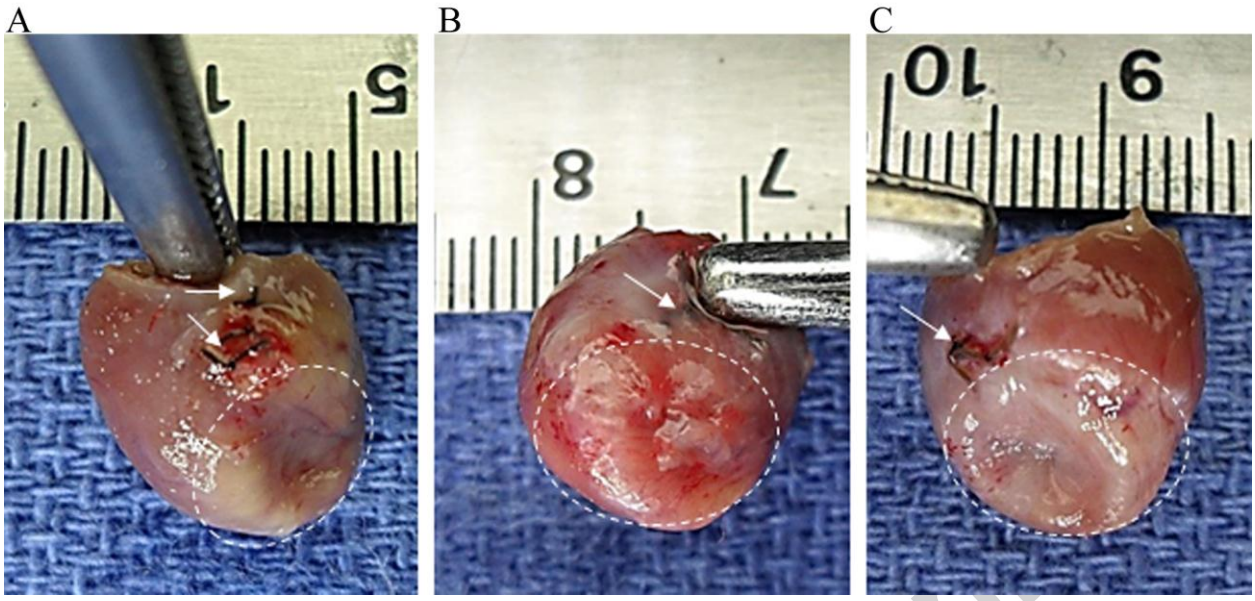

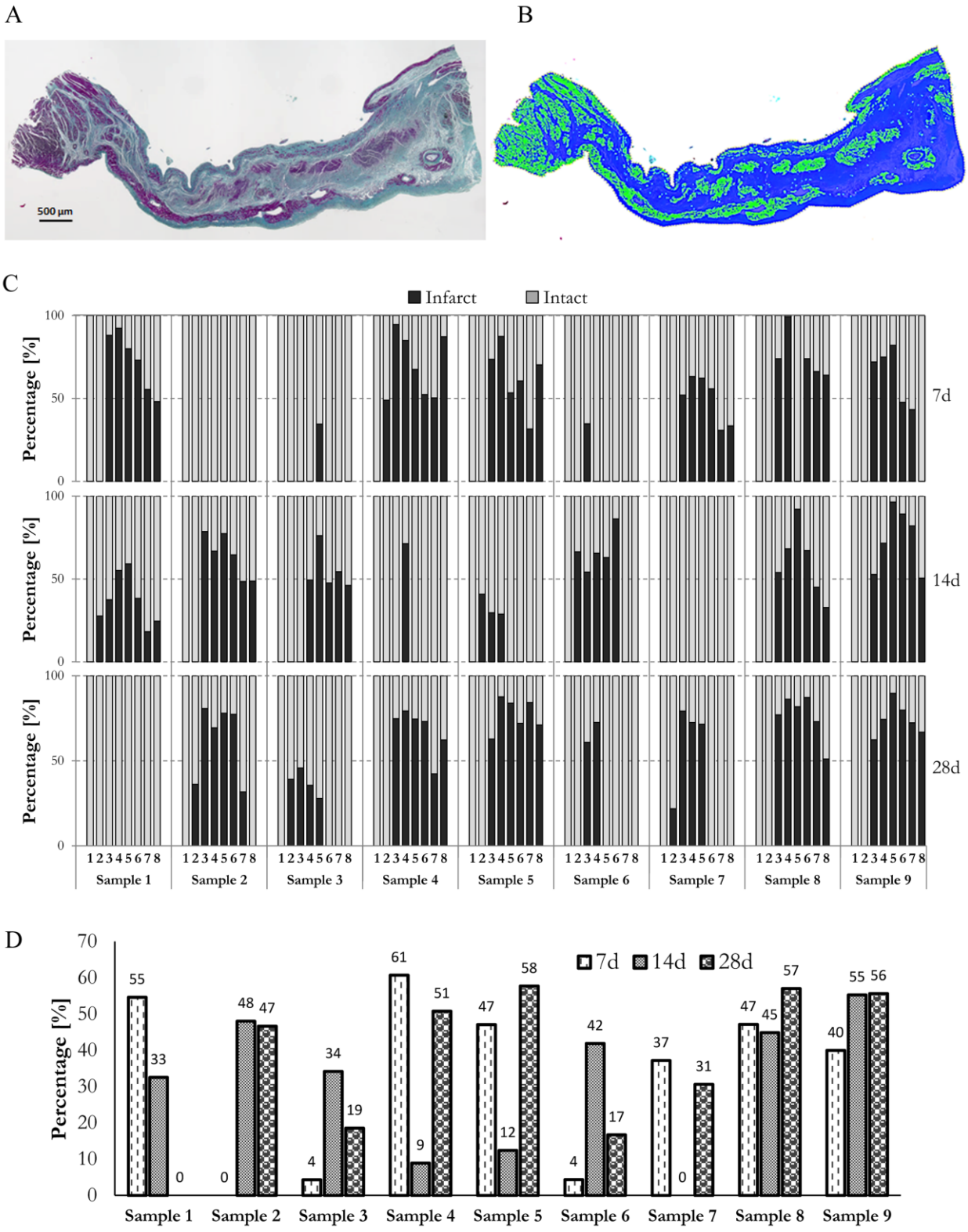

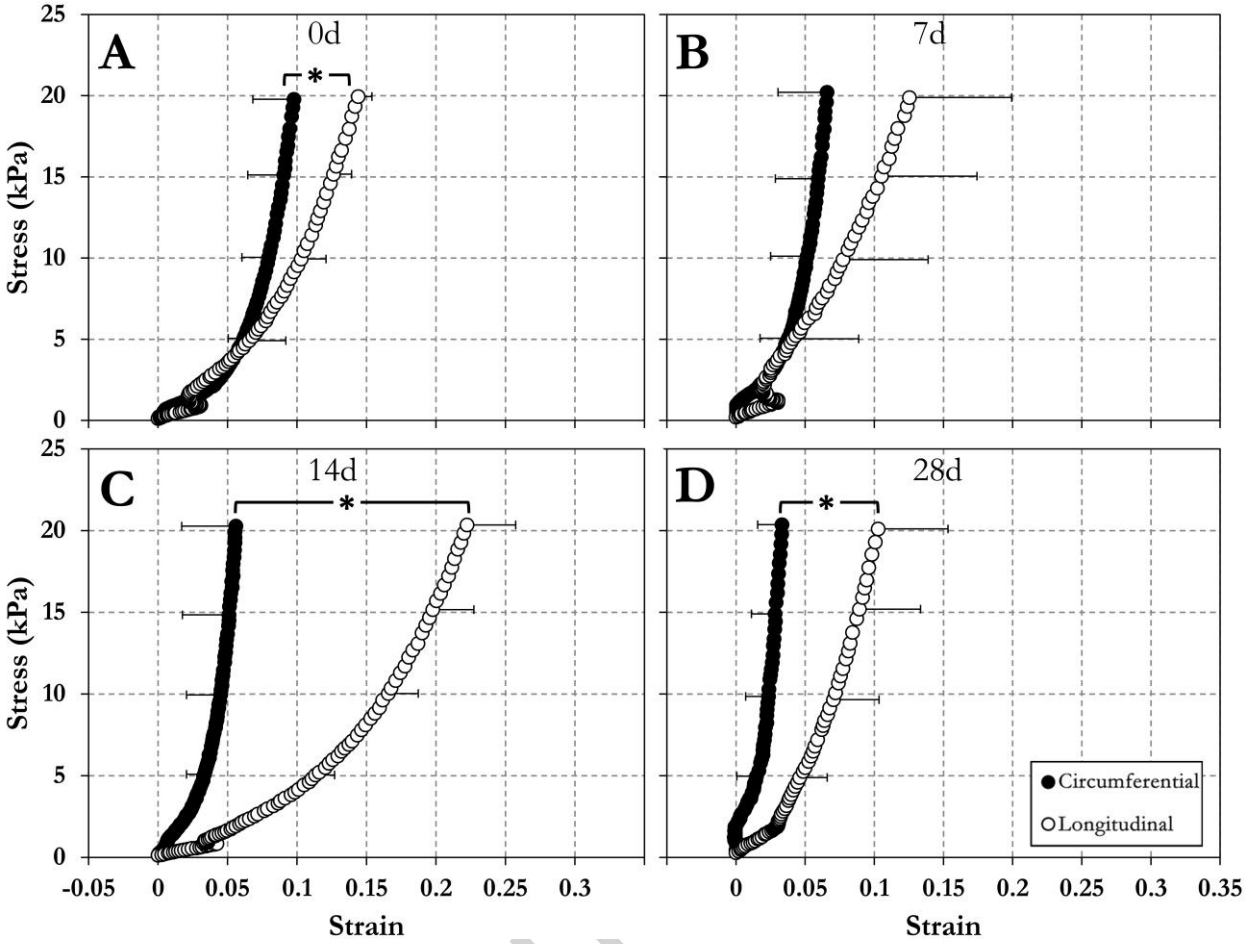

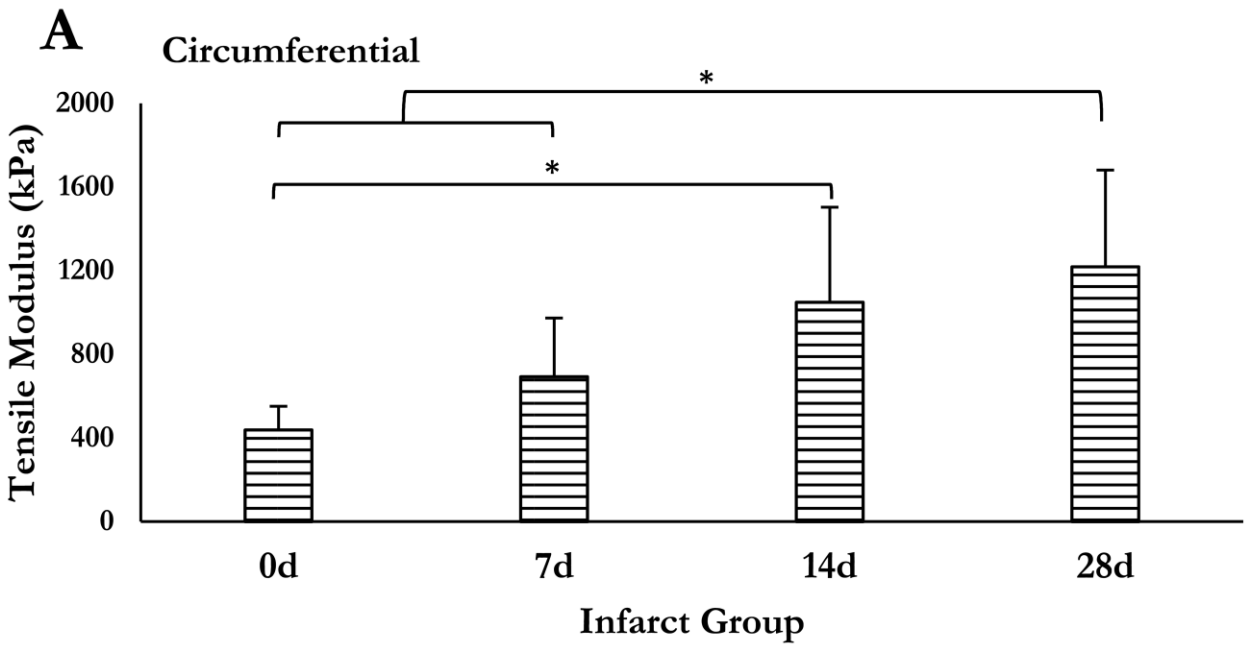

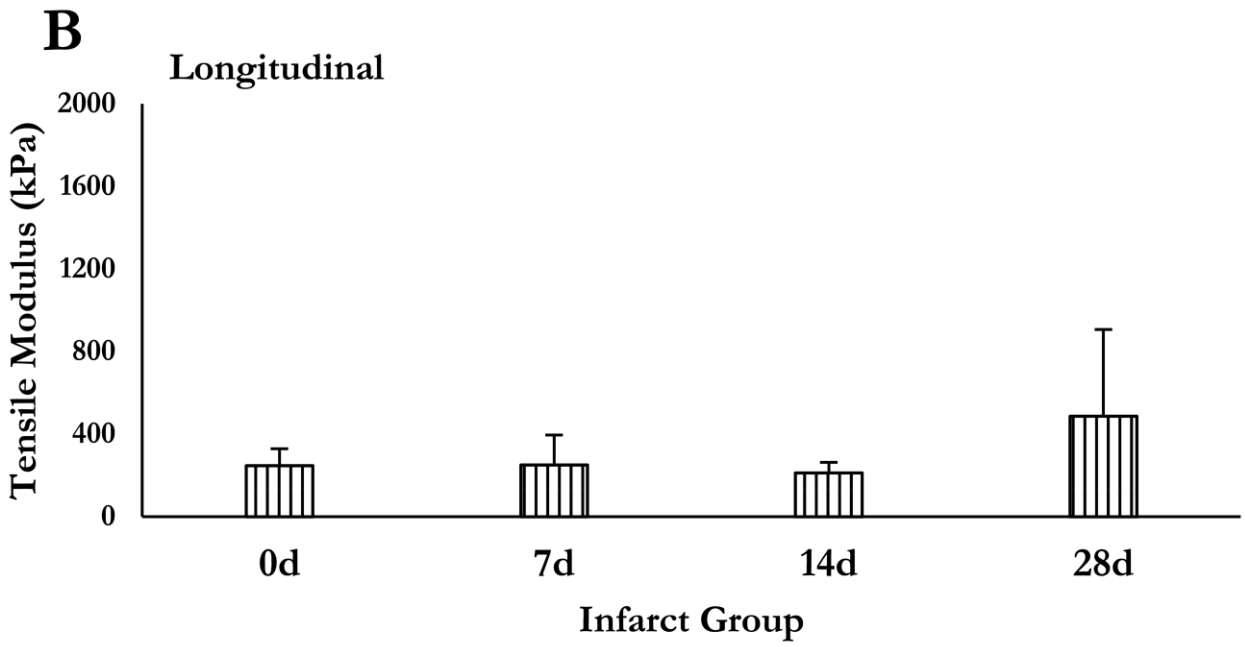

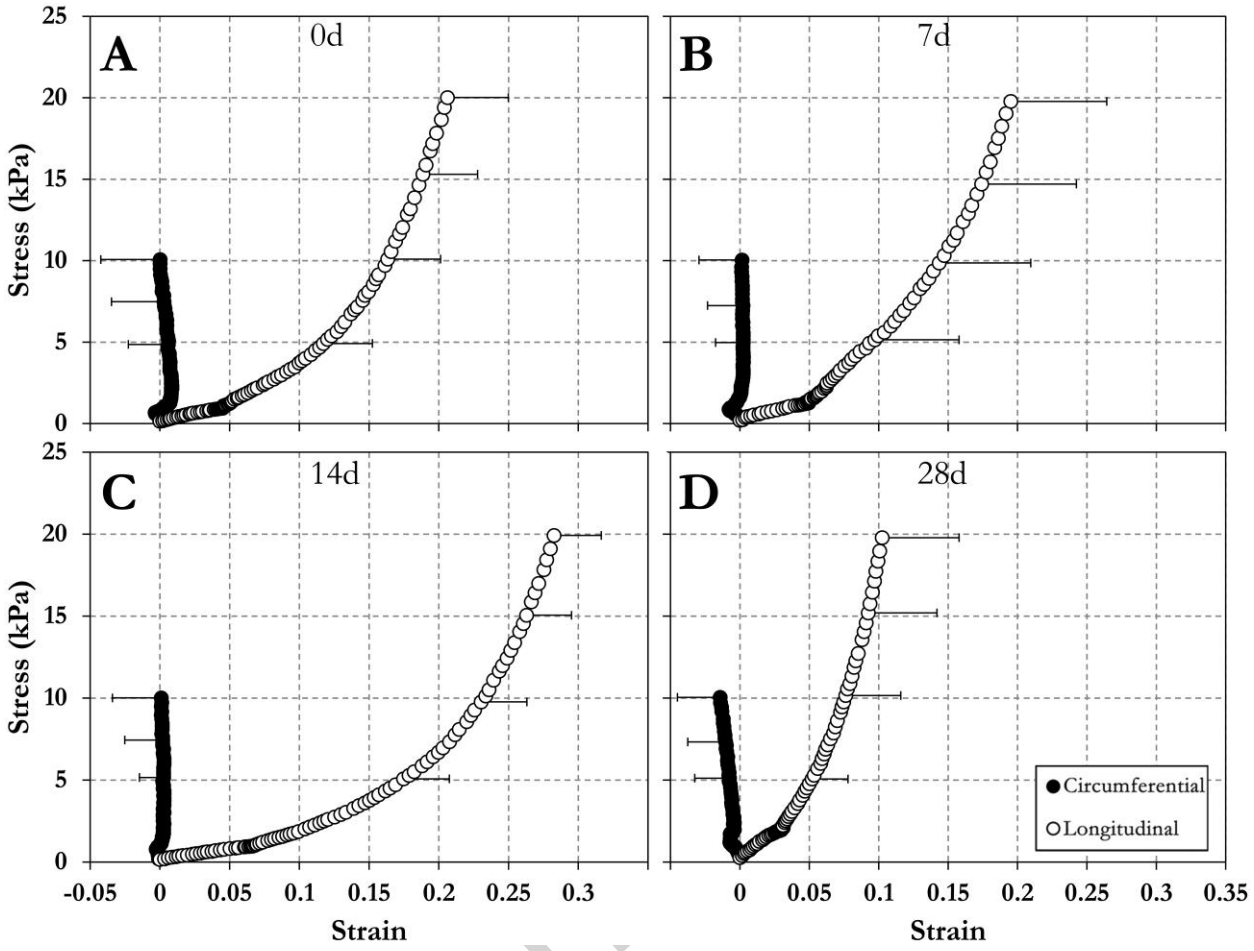

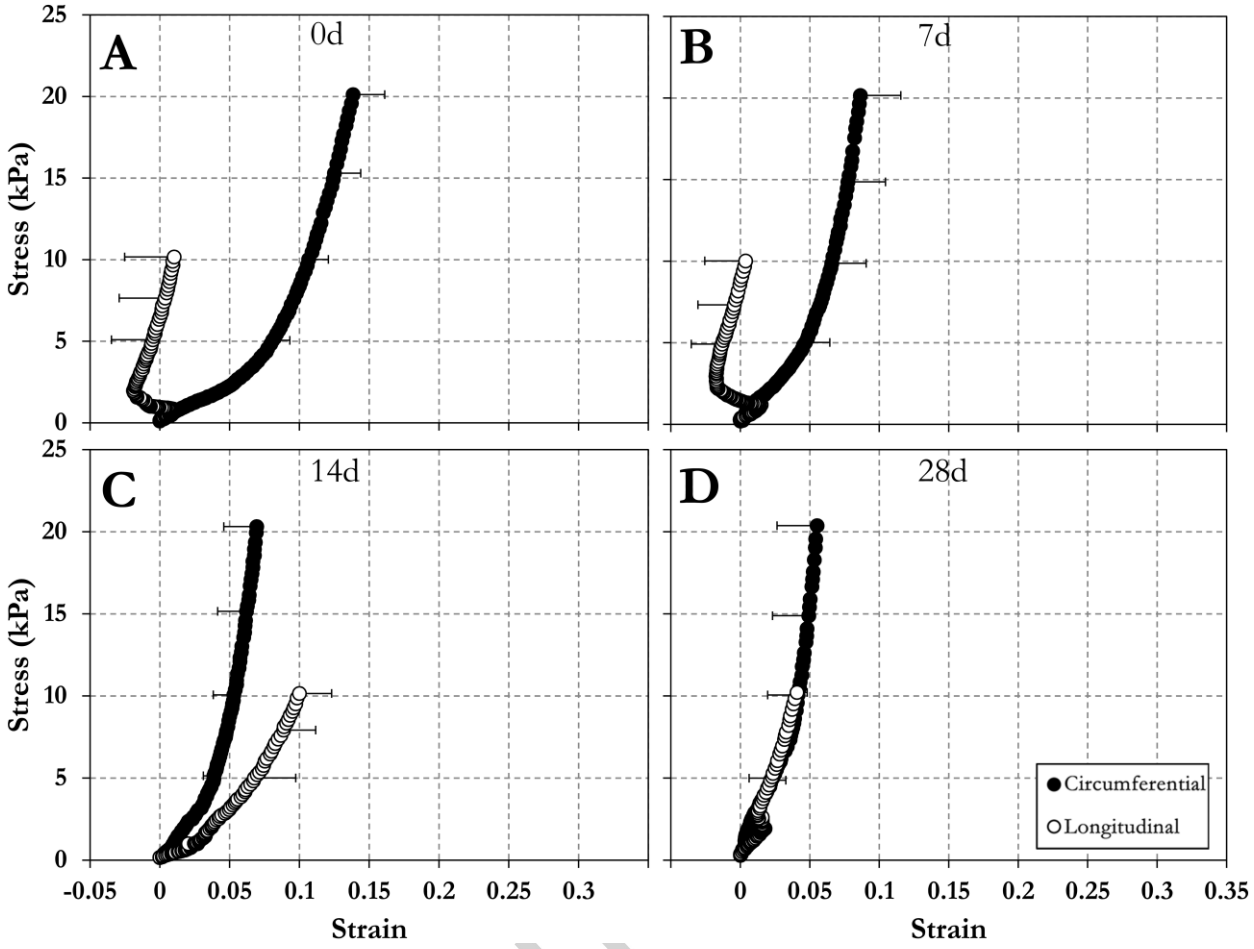

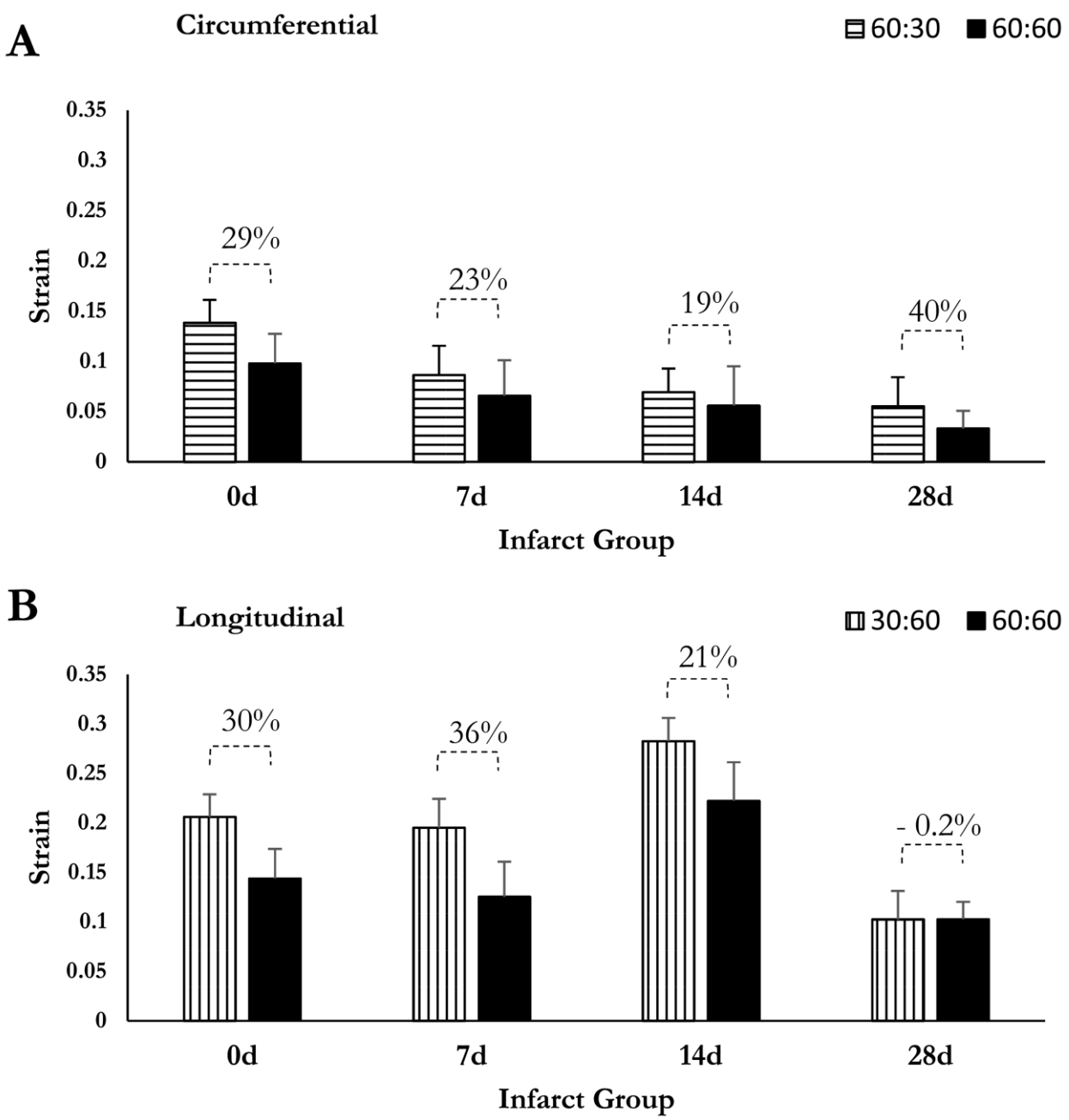

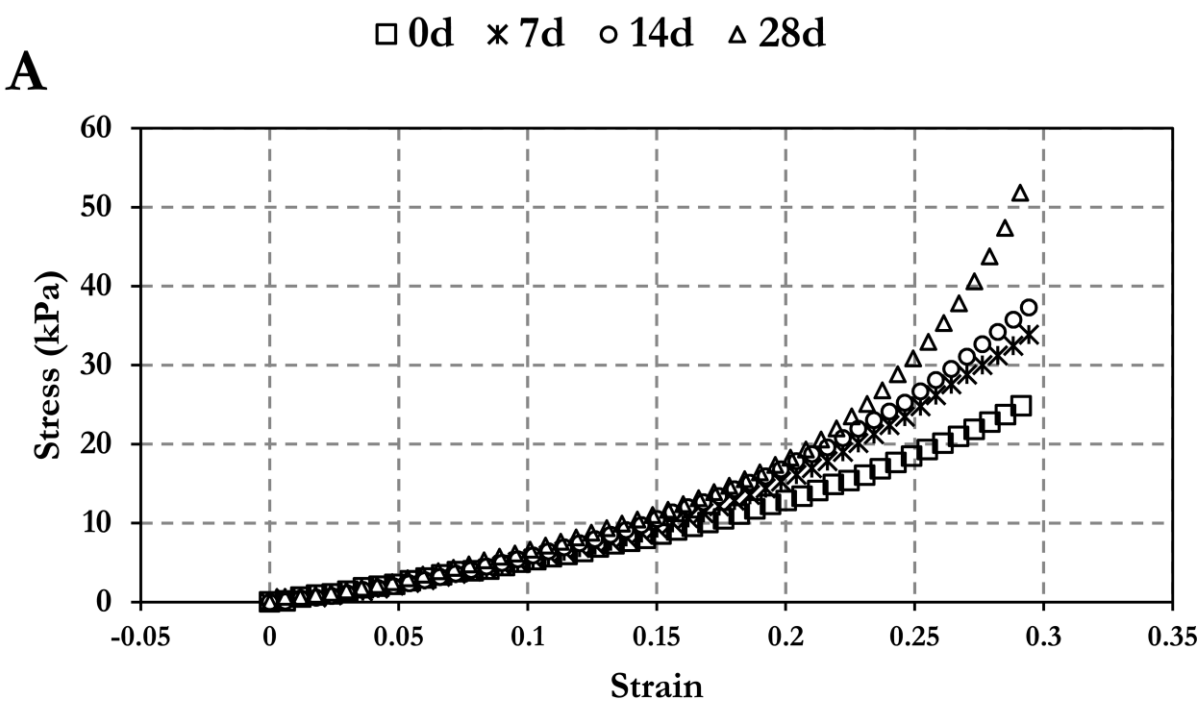

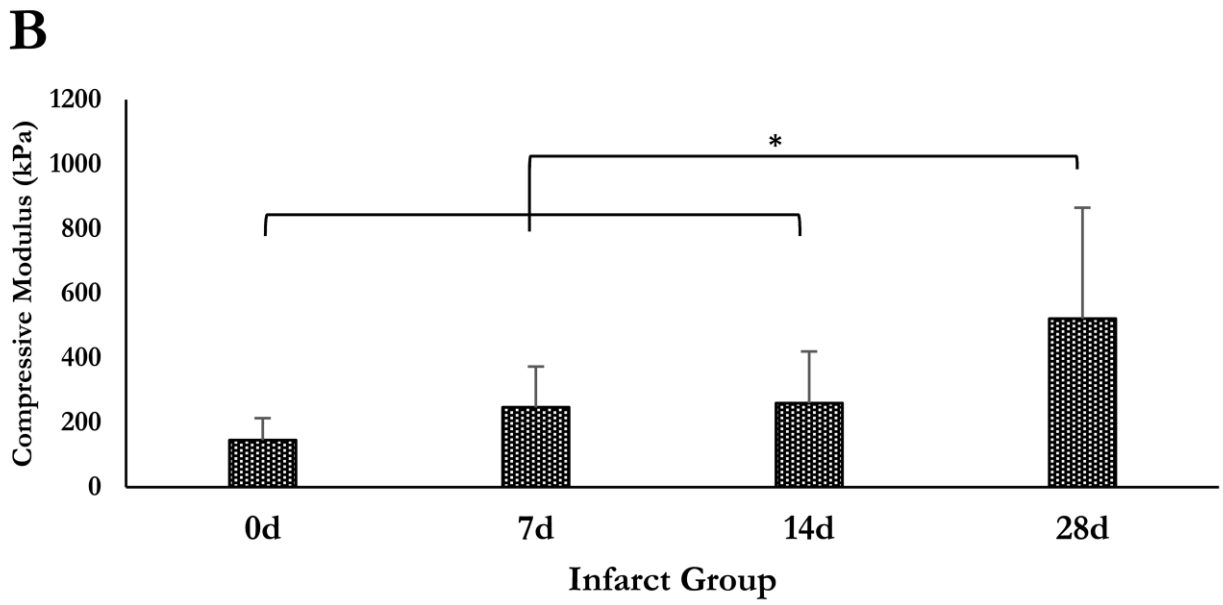

A

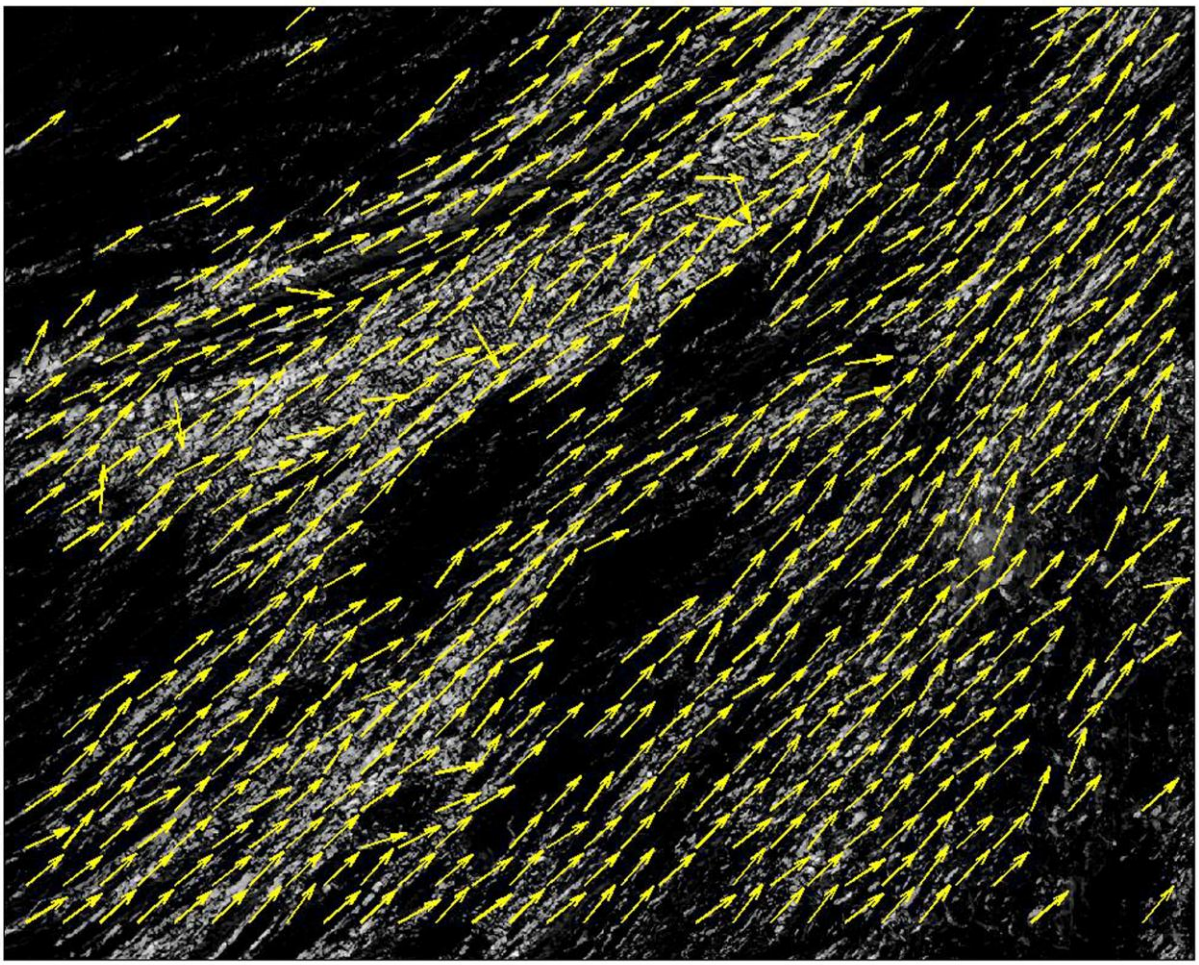

B

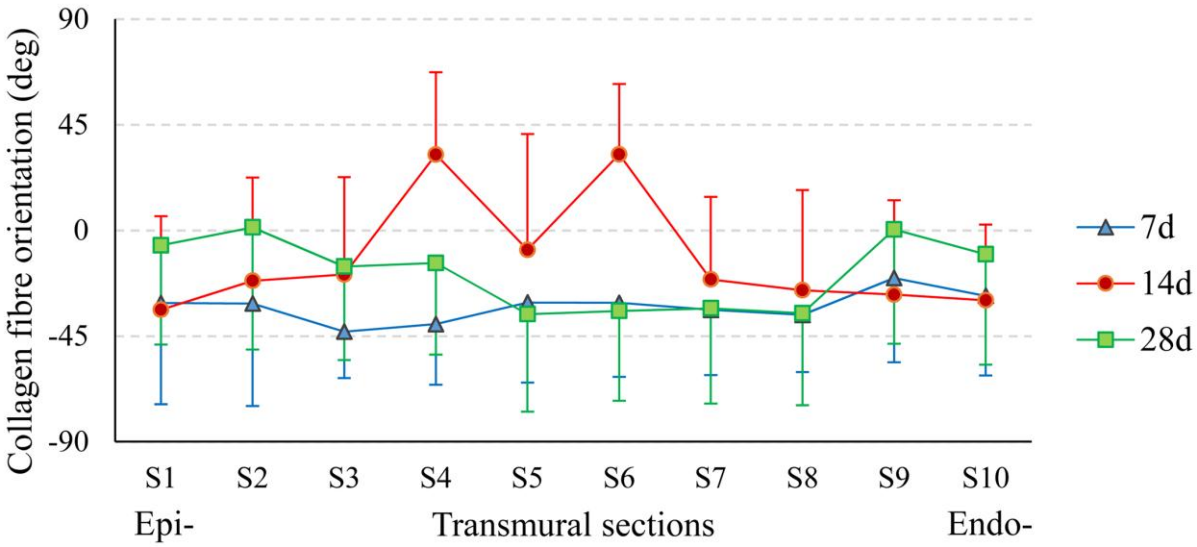

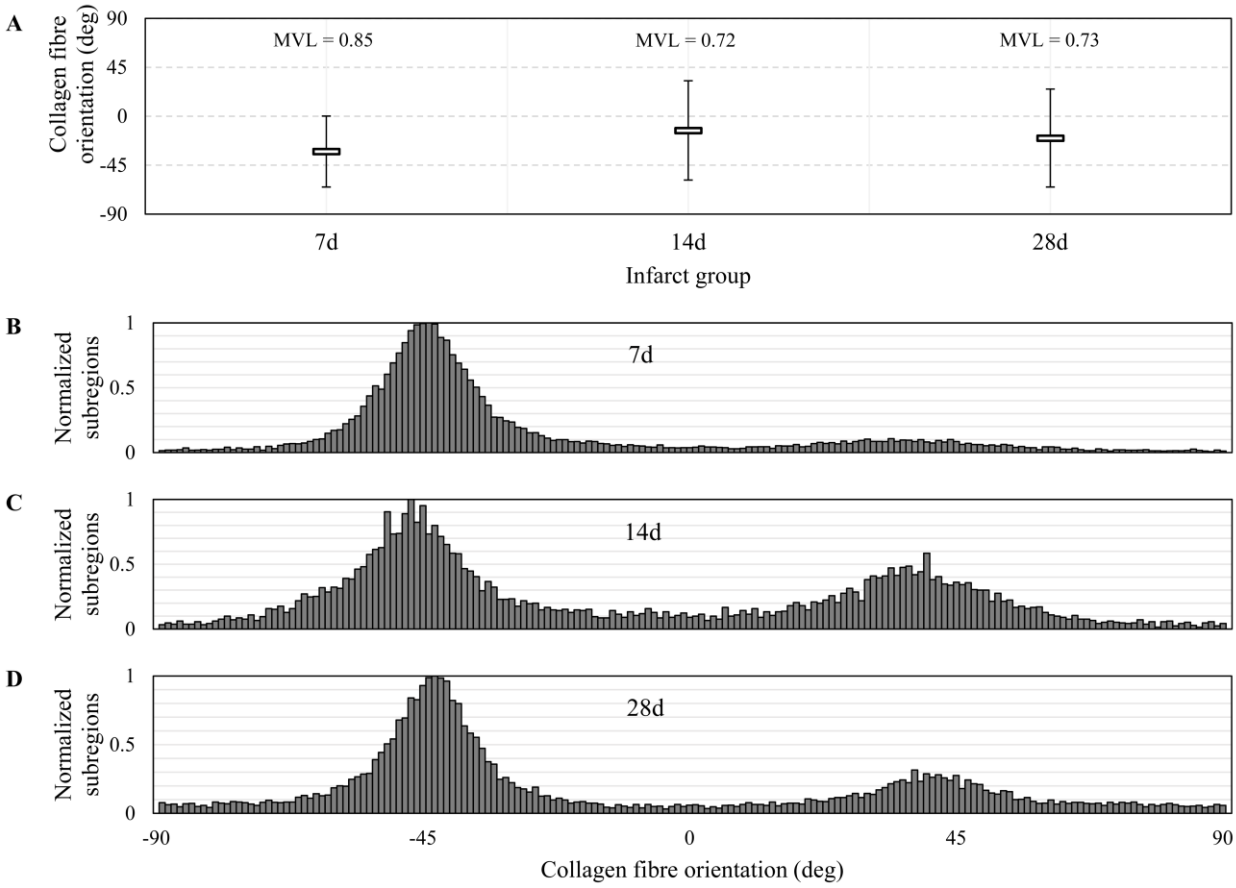

- Rat myocardial infarcts exhibit mechanical anisotropy up to 28 days post-infarction.
- Infarcts are stiffer in circumferential than in longitudinal direction.
- Mechanical anisotropy is supported by collagen fibre orientation in infarcts.
- Infarcts exhibit in-plane mechanical coupling.
- Circumferential and compressive stiffness of healing infarcts increases with time.